

Study of the Semidilute Solutions of Poly(*N,N*-dimethylacrylamide) by Fluorescence and Its Implications to the Kinetics of Coil-to-Globule Transitions

Kamdi Irondi, Mingzhen Zhang, and Jean Duhamel*

Institute for Polymer Research, Department of Chemistry, University of Waterloo, Waterloo, ON N2L 3G1, Canada

Received: September 30, 2005; In Final Form: December 1, 2005

The large scale motions of poly(*N,N*-dimethylacrylamide) chains randomly labeled with pyrene (Py–PDMA) were monitored by steady-state and time-resolved fluorescence in semidilute solutions of naked PDMA in acetone and DMF for polymer concentrations ranging from 0 to 550 g/L. Although increasing the polymer concentration of the solution led to a decrease of the mobility of the chromophore attached onto the PDMA backbone, this reduction was rather modest when compared to the large increase of the macroscopic viscosity. This result indicated that locally, the monomer constituting the chains experienced freedom of movement despite the high solution viscosity. The restricted mobility of the chromophore was characterized by the number of monomers occupying the volume probed by the excited chromophore during its lifetime, referred to as a fluorescence “blob”. The number of monomers constituting a fluorescence blob, $N_{F\text{-blob}}$, and the volume of a fluorescence blob, $V_{F\text{-blob}}$, were found to decrease as the polymer concentration of the solution increased, reflecting the decreased mobility experienced by the chromophore. In DMF, the radius of an F-blob was found to scale as $N_{F\text{-blob}}^\nu$, where ν equaled 0.66 ± 0.03 , very close to the expected value of the Flory exponent of 0.6 for a polymer in a good solvent. The combined knowledge of how $N_{F\text{-blob}}$ varies with the fluorescence lifetime of the chromophore and the coil density of the polymer was used to propose a new means of studying coil-to-globule transitions with potential implications for predicting the rate of protein folding.

Introduction

Short length scale motions of polymer chains provide information about polymer chain dynamics. They can be studied by a variety of techniques such as NMR,^{1–3} dielectric relaxation,^{4,5} or time-resolved optical spectroscopy^{6–10} under a variety of conditions either in solution^{3,10} or in the bulk.^{1,2,4–9} Information about polymer chain dynamics can also be inferred by monitoring the long length scale motions of polymer chains. Traditionally fluorescence quenching experiments, where a chromophore and its quencher both have been covalently attached at well-separated positions along a polymer chain, have proved a powerful tool to study long length scale motions of polymer chains.^{11–13} Such fluorescence experiments monitor the quenching events taking place between an excited chromophore and the quencher. These quenching events indicate that those monomers in the chain that bear the chromophore and its quencher have encountered, and since these encounters are controlled by the dynamics of the chain spanning the chromophore and quencher, the rate of quenching retrieved by the analysis of the fluorescence data provides information about the polymer chain dynamics. Because the chromophore pyrene in the ground state can quench an excited pyrene via the formation of an excimer, many fluorescence experiments have been carried out with pyrene since it acts as both a chromophore and a quencher, a major simplification in the chemistry associated with the labeling procedure.^{11–13}

Until 1999, the rate of quenching between an excited and a ground-state pyrene could be determined quantitatively only

when the polymer spanning the two pyrenes was monodisperse.¹⁴ In most instances, the end-to-end cyclization rate constant was measured for a monodisperse polymer labeled at both ends with pyrene.¹¹ The requirement of working with a monodisperse chain was necessary because the rate constant of excimer formation depends strongly on the chain length spanning the two pyrenes so that attaching pyrene at both ends of a polydisperse polymer or randomly along a polymer generates an intractable distribution of rate constants.^{15,16} Although the study of pyrene end-labeled monodisperse chains has provided a wealth of information on the dynamics of polymer chains in solution,¹¹ the study of the long length scale motions of polymers in semidilute solution with pyrene end-labeled monodisperse chains is complicated by the fact that the end-to-end cyclization rate constant decreases strongly with increasing chain length¹¹ and solvent viscosity.¹⁷ The important effect of entanglements in semidilute solutions can only be probed if the chain is long enough. In the case of pyrene end-labeled chains, this condition drastically decreases the number of end-to-end encounters between pyrenes making it difficult to measure accurately with a steady-state or time-resolved fluorometer. This detection problem is further accentuated by the viscosity increase associated with the increase in polymer concentration in semidilute solutions, which further reduces the number of end-to-end encounters.

In view of the above considerations, the fluorescence study of long length scale motions of polymers in a semidilute solution with polymer entanglements requires a long chain labeled with pyrenes located at positions separated by a distance shorter than the end-to-end distance of the polymer. More explicitly, the

* To whom correspondence should be addressed.

pyrene labels must be attached internally on the polymer. Most of these requirements were met in the study of a semidilute polystyrene solution performed more than 20 years ago with a 14K polystyrene exhibiting pyrene pendants evenly spaced every 25–30 monomer units as a collaboration between the Winnik and Guillet groups in Toronto.¹⁶ Unfortunately no quantitative information could be retrieved from this study because the analysis of the fluorescence decays could not be carried out with the then current understanding of excimer formation kinetics due to *multiple relaxation times due to excimer formation from pyrene pairs remote along the chain contour*.¹⁶ In other words, the pyrenes evenly spaced in the 1-D sequence of the polymer were randomly distributed in the 3-D volume of the polymer coil. The random distribution of the chromophores inside the volume occupied by the polymer coil resulted in a random distribution of distances between any two pyrene labels, which yielded the untractable distribution of encounter rate constants preventing the analysis of the fluorescence decays. This problem is actually analogous to the one encountered in proteomics¹⁸ where biochemists try to predict the 3-D structure of proteins from their 1-D sequence. Protein structure determination from the accurately established 1-D sequence remains a major challenge due to the random positioning of the amino acids inside the 3-D polypeptide coil at the early stages of folding.

The fluorescence blob model (FBM) introduced in 1999 by this laboratory allows one to circumvent the complications associated with the random positioning in solution of chromophores attached onto a polymer.¹⁴ In the FBM, a fluorescence blob, F-blob, is defined as the volume probed by a chromophore while it remains excited. The F-blob is a unit volume that can be used to divide the polymer coil, which becomes a cluster of F-blobs. Because the chromophore and its quencher are randomly distributed along the polymer backbone and inside the polymer coil, they can be assumed to distribute themselves randomly among the F-blobs according to a Poisson distribution. The kinetics of the encounters taking place between chromophores and quenchers can be derived by making an analogy with micellar systems.^{19,20} FBM analysis of the fluorescence decays of a polymer randomly labeled with pyrene yields the number of monomers constituting an F-blob, $N_{F\text{-blob}}$. Since a pyrene label attached onto a stiff or flexible polymer will probe a small or large F-blob during its lifetime, respectively, knowledge of $N_{F\text{-blob}}$ provides information about the flexibility and dynamics of the polymer. So far, the FBM has been applied to study the backbone dynamics of vinyl polymers randomly labeled with pyrene in dilute solutions.^{14,21,22} In the present work, the FBM is applied to three poly(*N,N*-dimethylacrylamide)s randomly labeled with pyrene (Py-PDMA) whose dynamics are investigated in semidilute solutions. These experiments were performed by mixing trace amounts of the pyrene labeled polymers with a large excess of unlabeled polymer to ensure that only intramolecular excimer formation is occurring. To the best of our knowledge, this work represents the first example where the long length scale motions of a polymer are being investigated quantitatively in the semidilute regime via a fluorescence quenching experiment.

Experimental Section

All chemicals were purchased from Sigma-Aldrich. The dialysis clips and bags used to purify the PDMA samples were purchased from VWR. All solvents were of spectrograde quality and Milli-Q water was used. The synthesis of all Py-PDMA samples used in this study has been reported earlier.^{21,22}

Synthesis of Poly(*N,N*-dimethylacrylamide). The unlabeled poly(*N,N*-dimethylacrylamide) (PDMA) was synthesized by radical polymerization. A volume of 65 mL of DMA (0.63 mole) was eluted through an inhibitor remover column three to four times and then placed in a flamed, dry, N₂-filled round-bottom flask that contained 29.5 mg of AIBN (1.79×10^{-4} mol) and 100 mL of DMF. The polymerization was carried out at 70 °C for 6 h after which the mixture was cooled to room temperature. Ice cold ethyl ether anhydrous (10× excess) was added to the reaction mixture to precipitate the polymer. The white precipitate was dried under vacuum. The polymer was dialyzed against water for 2 days with a 3500 MW cutoff dialysis bag to remove oligomers and residual DMF. The final product was obtained by freeze drying the dialyzed sample to remove water. The unlabeled polymer had a weight-average molecular weight (M_w) of 117K as determined by static light scattering.

Static Light Scattering. The M_w of the unlabeled PDMA sample (117K) was determined by static light scattering (SLS), using a dn/dc value of $0.084 \text{ mL} \cdot \text{g}^{-1}$, as determined with a Brice-Phoenix differential refractometer equipped with a 510 nm band-pass interference filter. All light scattering experiments were done in DMF. The SLS tubes (VWR) were flamed beforehand to remove eventual scratches in the glass and then washed for 30 min with an acetone fountain to remove dust. The polymer solutions were filtered through a $0.5 \mu\text{m}$ Teflon filter. The M_w of the unlabeled PDMA sample was then determined by Zimm plot extrapolation on a Brookhaven BI-200 SM light scattering goniometer equipped with a Lxel 2 W argon ion laser operating at 514.5 nm.

Intrinsic Viscosity Measurements. The viscosity of the polymer solutions was measured in DMF at 25 °C with an Ubbelohde viscometer in a thermostated water bath.

Sample Preparation for Fluorescence Experiments. The samples containing 0–550 g/L unlabeled PDMA were prepared by weighing the required amount of unlabeled PDMA in a vial and adding to the vial a measured quantity of a solution of Py-PDMA with an optical density at 344 nm of 0.1, ensuring that the pyrene concentration in the solutions was always smaller than $3 \times 10^{-6} \text{ M}$. The solution was stirred for at least 4 h until the polymer was completely dissolved. The volume of the PDMA solution was determined as follows. Water was added to a second vial until the meniscus of the water matched that of the vial containing the PDMA solution. The mass of water added to the second vial was determined and transformed into a volume by using the density of water at 25 °C. This volume was taken as that of the n PDMA solution. This procedure allowed us to report the polymer concentration in the solutions in units of g/L instead of the units of wt % more usually found in the literature. Samples with concentrations between 0 and 200 g/L were degassed by bubbling N₂ into the solution for 20 min, while samples with higher polymer concentrations and higher viscosity were degassed by 5 to 6 successive freeze–thaw cycles and then sealed under vacuum.

Steady-State Fluorescence Measurements. Fluorescence spectra of the samples were obtained with a Photon Technology International LS-100 steady-state system and all measurements were done with the right angle geometry. The samples were excited at 344 nm and the monomer (I_M) and excimer (I_E) fluorescence intensities were obtained by integrating the fluorescence spectra over a range of 372–378 nm for the monomer and from 500 to 530 nm for the excimer.

Time-Resolved Fluorescence Measurements. The fluorescence decay curves for the samples were obtained with a Photochemical Research Associates Inc. System 2000. The

excitation wavelength was set at 344 nm and the fluorescence decays of the pyrene monomer were acquired at 375 nm. A cutoff filter at 370 nm was used on the emission side to prevent eventual scattered light from reaching the detector. All fluorescence decays were acquired over 512 channels and had 20 000 counts at the decay maximum. The instrument and decay acquisition have been described in more details in earlier publications.^{14,21,22}

Analysis of the Fluorescence Decays. The fluorescence decays of the pyrene monomer were analyzed with eq 1, which handles the Fluorescence Blob Model (FBM).¹⁴ In eq 1, the parameters A_2 , A_3 , and A_4 are related to the pseudo-unimolecular rate constant of excimer formation between one excited pyrene and one ground-state pyrene located in the same F-blob, k_{F-blob} , the average number of pyrenes per F-blob, $\langle n \rangle$, and the product $k_e[F-blob]$ where k_e is the rate constant for exchange of ground-state pyrenes from one F-blob to another and $[F-blob]$ represents the local concentration of F-blobs inside the polymer coil. Tachiya's mathematical treatment was used to derive eq 1.¹⁹

$$[Py^*]_{(t)} = f \exp \left[- \left(A_2 + \frac{1}{\tau_M} \right) t - A_3 (1 - \exp(-A_4 t)) \right] + (1 - f) \exp(-t/\tau_M) \quad (1)$$

The parameters A_2 , A_3 , and A_4 are described in eq 2.

$$A_2 = \langle n \rangle \frac{k_{F-blob} k_e [F-blob]}{k_{F-blob} + k_e [F-blob]}$$

$$A_3 = \langle n \rangle \frac{k_{F-blob}^2}{(k_{F-blob} + k_e [F-blob])^2}$$

$$A_4 = k_{F-blob} + k_e [F-blob] \quad (2)$$

Equations 1 and 2 have expressions which are similar to those used to deal with the diffusion-controlled encounters between an excited chromophore and its quencher in micellar systems.²⁰

In eq 1, τ_M represents the lifetime of the unquenched pyrene monomer. It was measured with a Py-PDMA sample containing a very low pyrene content and found to equal 256 ns in acetone and 220 ns in DMF, regardless of polymer concentration. The value of τ_M was fixed in the analysis. At low pyrene content, a substantial fraction of the pyrene pendants are too far apart to form an excimer and these pyrenes emit with the lifetime τ_M . This fraction is given by the preexponential factor $1 - f$ in eq 1. The other pyrenes represented by the fraction f form excimer and their behavior is described by the first exponential in eq 1. Fitting the fluorescence decays of the pyrene monomers with eq 1 yields the parameters k_{F-blob} , $\langle n \rangle$, and $k_e[F-blob]$. $\langle n \rangle$ can be used to determine the number of monomer units in an F-blob, N_{F-blob} , with eq 3.

$$N_{F-blob} = \frac{\langle n \rangle}{(\lambda/f) \times (285x + 99(1 - x))} \quad (3)$$

In eq 3, λ is the pyrene content of the polymer expressed in moles of pyrene per gram of polymer, x represents the molar fraction of labeled monomers in the polymer chain, 285 g/mol represents the molar mass of a pyrene-labeled monomer unit, and 99 g/mol is the molar mass of an unlabeled monomer. N_{F-blob} is used as a measure of the dimension of an F-blob.

Results

The fluorescence experiments were performed with three Py-PDMAs having pyrene contents of 265, 385, and 570 μmol of

TABLE 1: Weight-Average Molecular Weights and Pyrene Contents of PDMA Samples

sample	M_w , 10^3 g/mol	pyrene content, λ , $\mu\text{mol/g}$
nPDMA	117	0
P265	165	265
P385	134	385
P570	105	570

pyrene per gram of polymer. These samples are referred to as P265, P385, and P570, respectively. Their M_w value and pyrene content are listed in Table 1. The concentration of the Py-PDMAs in solution is such that the pyrene concentration in all experiments equals 2.5×10^{-6} M. This pyrene concentration is equivalent to polymer concentrations of 9.4, 6.5, and 4.4 mg/L for P265, P385, and P570, respectively. The nonlabeled PDMA, nPDMA, of weight average molecular weight 117K was mixed with the Py-PDMA solutions. Since PDMA is transparent where pyrene absorbs and emits, the fluorescence emitted by the few Py-PDMA molecules dissolved in a sea of PDMA reports on the process of excimer formation occurring intramolecularly inside single Py-PDMA coils. Acetone and *N,N*-dimethylformamide (DMF) were chosen to perform these fluorescence experiments because they have been shown to be respectively a poor (θ) and good solvent for Py-PDMA at room temperature.^{21,22} The overlap concentration, C^* , of nPDMA was found to equal 42 and 26 g/L in acetone and DMF indicating that any fluorescence experiment performed at a polymer concentration larger than C^* is done in the semidilute regime. C^* was obtained by taking the inverse of the intrinsic viscosity measured with an Ubbelohde viscometer.²³

The fluorescence spectra of all Py-PDMAs were acquired as a function of nPDMA concentration. They are shown in Figure 1 for all Py-PDMAs in DMF. The spectra were normalized at the 0–0 peak at 374 nm. For all Py-PDMA samples regardless of solvent or pyrene content, the excimer fluorescence decreased with increasing nPDMA concentration. From these fluorescence spectra, the ratio of the fluorescence intensity of the excimer to that of the monomer, the I_E/I_M ratio, was determined. The I_E/I_M ratio decreased with increasing nPDMA concentration. Although the I_E/I_M ratio increased with increasing pyrene content at any given nPDMA concentration, the I_E/I_M vs [nPDMA] profiles looked very similar. Indeed if all I_E/I_M ratios of P265 in DMF were divided by those of P385 in DMF obtained at similar nPDMA concentrations, an average ratio of 0.67 ± 0.05 was obtained. Similar observations could be made for all I_E/I_M data sets obtained with different polymers in either acetone or DMF. Multiplying the I_E/I_M ratios of P265, P385, and P570 by a normalization factor of 1.00, 0.67, and 0.37 in DMF and 1.00, 0.54, and 0.25 in acetone, respectively, resulted in overlapping trends, as shown in Figure 2. Figure 2 suggests that the phenomenon that induces the drop in I_E/I_M is not due to changes in the pyrene contents of the Py-PDMA samples since the I_E/I_M trends overlap in a given solvent regardless of pyrene content, but rather to a change in the mobility of the chromophores when the nPDMA concentration is increased. The main difference in the trends obtained in DMF (Figure 2A) and acetone (Figure 2B) is that I_E/I_M decreases with increasing nPDMA concentration much more quickly in acetone (a poor solvent for Py-PDMA) than in DMF (a good solvent for Py-PDMA).^{21,22} In Figure 2A, the viscosity of polymer solutions in DMF is plotted as a function of polymer concentration. The striking effect observed in Figure 2A is that the I_E/I_M ratio decreases by only 35% as the nPDMA concentration increases from 0 to 330 g/L, while the macroscopic viscosity

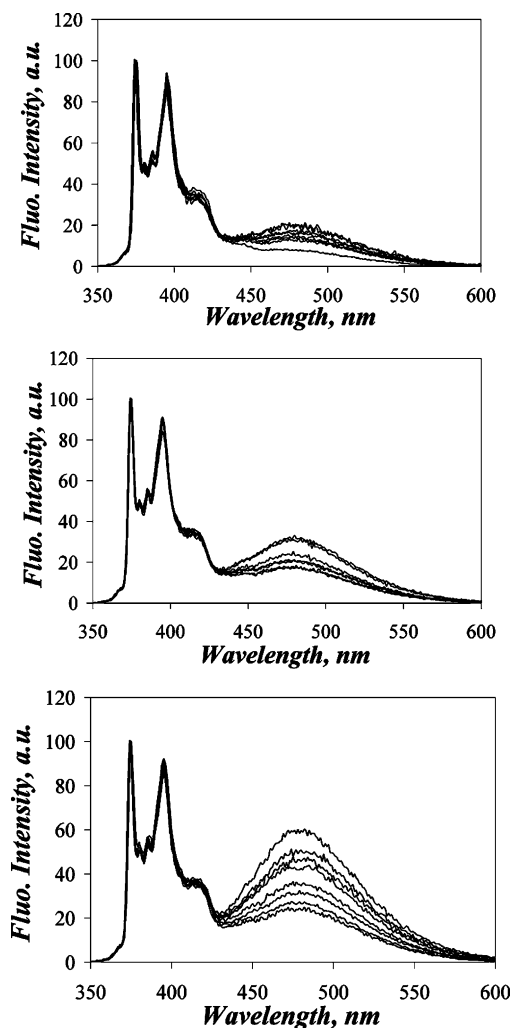


Figure 1. Fluorescence spectra of P265 (top), P385 (middle), and P570 (bottom) excited at 344 nm. In each panel, the polymer concentration is increased from 0 (top trace) to 550 g/L (bottom trace). All spectra were normalized at the 0–0 peak of the pyrene monomer located at 374 nm.

measured with an Ubbelohde viscometer increases 300-fold from 0.85 to 290 mPa·s over the same range of *n*PDMA concentration. Since the I_E/I_M ratio of a pyrene-labeled polymer is inversely proportional to the solvent viscosity,¹⁷ a 300-fold increase in solvent viscosity should result in a 300-fold decrease in the I_E/I_M ratio. The fact that this drastic decrease in I_E/I_M is not observed in DMF demonstrates that locally, the chains exhibit significant freedom of motion allowing substantial excimer formation at polymer concentrations as high as 550 g/L. Similarly, the I_E/I_M ratio decreases by only 60% in acetone when the *n*PDMA concentration is increased from 0 to 300 g/L. The observation that the I_E/I_M ratio of Py–PDMA in DMF (a good solvent for Py–PDMA) decreases little with increasing polymer concentration is not an isolated example. A similar observation was made by Winnik and Guillet for a pyrene-labeled polystyrene sample in toluene.¹⁶

The fluorescence decays of the pyrene monomer of the Py–PDMA solutions were acquired with increasing *n*PDMA concentrations. As shown in Figure 3 for P385 in acetone, as the *n*PDMA concentration increased, the pyrene monomers became longer lived, reflecting the increasingly hindered mobility of the pyrene label. Fitting the pyrene monomer fluorescence decays of P265, P385, and P570 in DMF and acetone with *n*PDMA concentrations ranging from 0 to 550 g/L

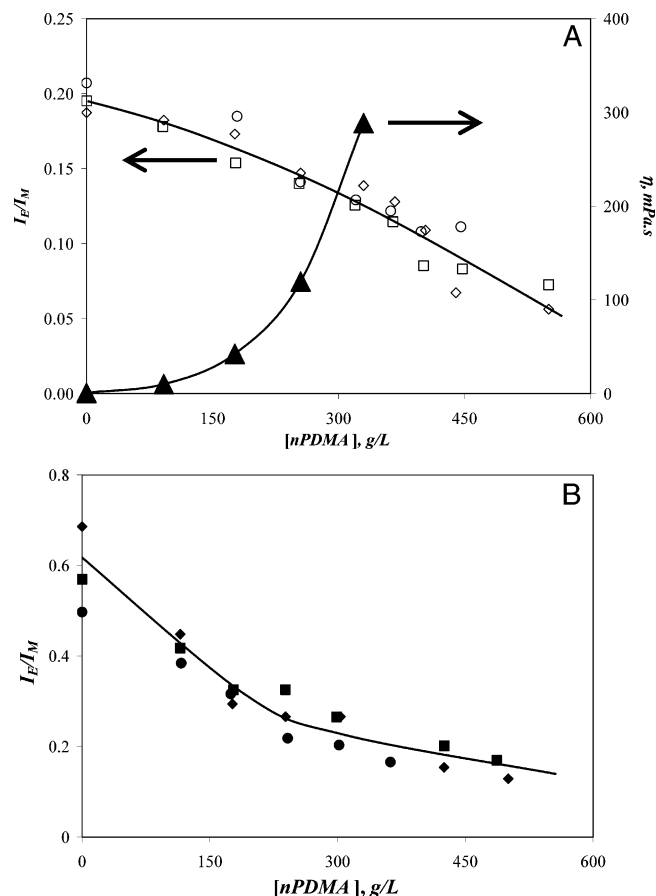


Figure 2. (A) Plot of the I_E/I_M ratio (left axis) as a function of *n*PDMA concentration for P265 (◇), P385 (○), and P570 (□) in DMF normalized by the factor 1.00, 0.67, and 0.37, respectively. Plot of the solution viscosity (right axis) as a function of *n*PDMA concentration. (B) Plot of the I_E/I_M ratio as a function of *n*PDMA concentration for P265 (◇), P385 (●), and P570 (■) in acetone normalized by the factor 1.00, 0.54, and 0.25, respectively.

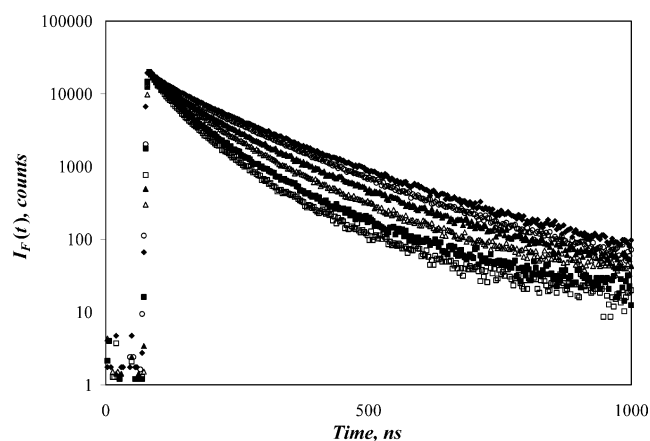


Figure 3. Fluorescence decays of P385 in acetone acquired at $\lambda_{ex} = 344$ nm and $\lambda_{em} = 375$ nm for *n*PDMA concentrations of 0, 116, 175, 241, 302, 362, 424, and 485 g/L from bottom to top.

with eq 1 according to the fluorescence blob model (FBM) yielded the average number of pyrenes per blob, $\langle n \rangle$, and the quenching rate constant, k_{F-blob} , between an excited pyrene monomer and a single ground-state monomer located inside the same F-blob. In turn, the number of monomer units constituting an F-blob, N_{F-blob} , could be determined by introducing $\langle n \rangle$ into eq 3. The parameters retrieved from the analysis of the decays in acetone and DMF with eq 1 are listed in the Supporting

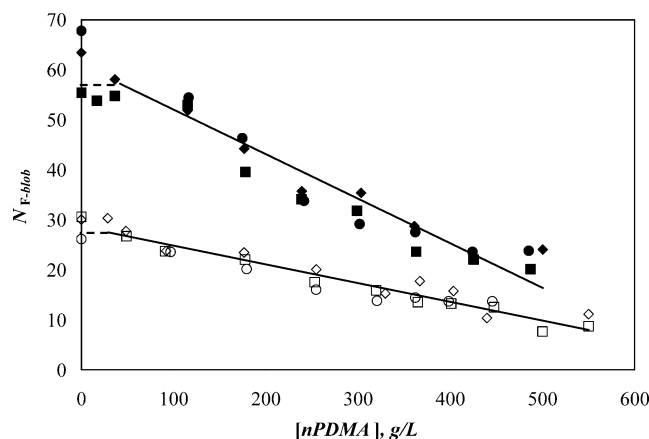


Figure 4. Plot of $N_{F\text{-blob}}$ as a function of $n\text{PDMA}$ concentration for P265 (\diamond , \blacklozenge), P385 (\circ , \bullet), and P570 (\square , \blacksquare) in DMF (empty symbols) and acetone (full symbols).

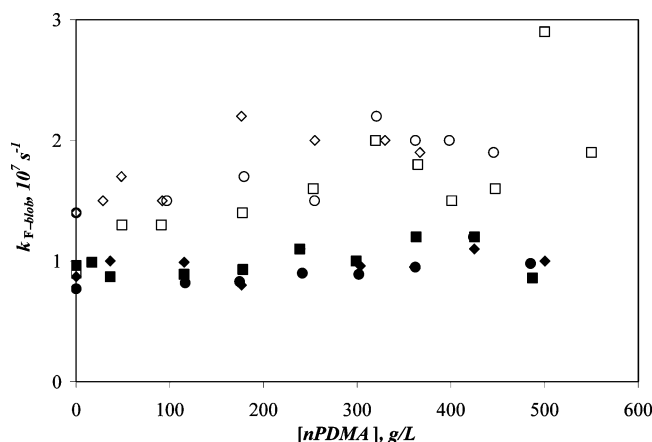


Figure 5. Plot of $k_{F\text{-blob}}$ as a function of $n\text{PDMA}$ concentration for P265 (\diamond , \blacklozenge), P385 (\circ , \bullet), and P570 (\square , \blacksquare) in DMF (empty symbols) and acetone (full symbols).

Information in Tables SI.1 and SI.2, respectively. The fits were good with all χ^2 values being smaller than 1.29 and the residuals and the autocorrelation function of the residuals randomly distributed around zero. $N_{F\text{-blob}}$ and $k_{F\text{-blob}}$ were plotted as a function of $n\text{PDMA}$ concentration in Figures 4 and 5, respectively. The first observation to be made in Figures 4 and 5 is that within experimental error, the trends shown do not depend on the pyrene content of the Py-PDMA samples, which demonstrates that the FBM accounts satisfyingly for the changes in pyrene content when analyzing the fluorescence decays of polymers randomly labeled with pyrene in the semidilute regime. In both DMF and acetone, $N_{F\text{-blob}}$ decreases monotonically with increasing $n\text{PDMA}$ concentration. These trends are reasonable because an F-blob has been defined as the volume probed by an excited chromophore during its lifetime. As the $n\text{PDMA}$ concentration increases, the chains become entangled and their local mobility decreases. The excited chromophore probes a smaller volume reflected by the smaller $N_{F\text{-blob}}$ values. Nevertheless, the loss in local mobility is rather limited compared with the enormous increase in macroscopic viscosity (cf. Figure 2). By increasing the $n\text{PDMA}$ concentration from 0 to 330 g/L, the macroscopic viscosity of the DMF solution increases 300-fold whereas $N_{F\text{-blob}}$ is only halved in either DMF or acetone. This result confirms the observation made in Figure 2 that the I_E/I_M ratio does not change much with increasing viscosity due to the mobility experienced locally by the 1-pyrenyl pendants. It is also interesting to note that regardless of $n\text{PDMA}$ concentration, the $N_{F\text{-blob}}$ value obtained in acetone is always

larger than that in DMF. This effect is attributed to the lower viscosity of acetone ($\eta_{\text{acetone}}^{25^\circ\text{C}} = 0.306 \text{ mPa}\cdot\text{s}$, $\eta_{\text{DMF}}^{25^\circ\text{C}} = 0.794 \text{ mPa}\cdot\text{s}$) and the longer lifetime of the 1-pyrenyl pendant in acetone ($\tau_M(\text{acetone}) = 256 \text{ ns}$, $\tau_M(\text{DMF}) = 220 \text{ ns}$). Both variables allow the excited pyrene to probe a larger volume during its lifetime resulting in a larger $N_{F\text{-blob}}$ in acetone.

In Figure 5, the rate constant, $k_{F\text{-blob}}$, is found to remain constant within experimental error with $n\text{PDMA}$ concentration in acetone and DMF and equals $1.0 \pm 0.1 \times 10^7$ and $1.7 \pm 0.6 \times 10^7 \text{ s}^{-1}$, respectively. The constancy of $k_{F\text{-blob}}$ in acetone and DMF with $n\text{PDMA}$ concentration is expected. As explained in an earlier publication, $k_{F\text{-blob}}$ is a pseudo-unimolecular rate constant.²¹ It is the product of the rate constant for the diffusion-controlled bimolecular encounter between two pyrenes, k , with the concentration equivalent to one ground-state pyrene inside an F-blob, $1/V_{F\text{-blob}}$. As the $n\text{PDMA}$ concentration increases, the local solution viscosity increases and k decreases since the rate constant for diffusion-controlled encounters is inversely proportional to the solution viscosity.¹⁷ As the local solution viscosity increases, the volume probed by an excited pyrene, $V_{F\text{-blob}}$, decreases and $1/V_{F\text{-blob}}$ increases. The decrease in k and the increase in $1/V_{F\text{-blob}}$ are expected to counterbalance one another as found for $k_{F\text{-blob}} = k \times 1/V_{F\text{-blob}}$ in Figure 5 for acetone and DMF. The $k_{F\text{-blob}}$ value was found to exhibit a larger scatter in DMF. The reason why the parameters reporting on the kinetics of excimer formation are more scattered in DMF than in acetone lies in the fact that Py-PDMA yields less excimer in DMF (good solvent) than in acetone (poor solvent). This results in a fraction of the pyrene monomers forming excimer by diffusion, f , which is always substantially larger in acetone than in DMF, especially for the Py-PDMA sample having the lowest pyrene content, namely P265. Since a good accuracy of the retrieved parameters in eq 1 is usually achieved when f is larger than 0.90, it is clear from Table SI.2 that a poorer accuracy and a larger scatter is expected from the data obtained in DMF, as shown in Figure 5.

One interesting consequence of working with semidilute polymer solutions is that above C^* , the polymer concentration can be assumed to be the same throughout the solution. This leads to $V_{F\text{-blob}}$ being equal to $N_{F\text{-blob}}M(\text{DMA})/[n\text{PDMA}]$ for $n\text{PDMA}$ concentrations larger than C^* , where C^* has been found to equal 42 and 26 g/L in acetone and DMF, respectively. $M(\text{DMA})$ represents the molar mass of an *N,N*-dimethylacrylamide monomer and is equal to 99 g/mol. The radius of an F-blob, $R_{F\text{-blob}}$, was calculated assuming the geometry of an F-blob to be that of a sphere. A plot of $R_{F\text{-blob}}$ as a function of $[n\text{PDMA}]$ is shown in Figure 6. This plot represents the first example where the volume probed by an excited pyrene attached onto a polymer in solution is measured quantitatively. For both acetone and DMF, $R_{F\text{-blob}}$ decreases monotonically with increasing polymer concentration. This is expected since the increased amount of polymer present in the solution hinders the motion of the excited chromophore. Within experimental error, the trends shown in Figure 6 do not depend on the pyrene content of the polymer, which demonstrates that the phenomenon being monitored depends uniquely on the polymer and not on the amount of fluorescent probe attached onto the backbone. According to the data shown in Figure 6, $R_{F\text{-blob}}$ is substantially larger in acetone than in DMF. Within the framework of the FBM, $V_{F\text{-blob}}$ should be proportional to the lifetime of the chromophore (256 and 220 ns in acetone and DMF, respectively) and inversely proportional to the viscosity of the solvent (0.306 and 0.794 mPa·s for acetone and DMF at 25 °C, respectively). Just like $N_{F\text{-blob}}$ in Figure 4, the effects of

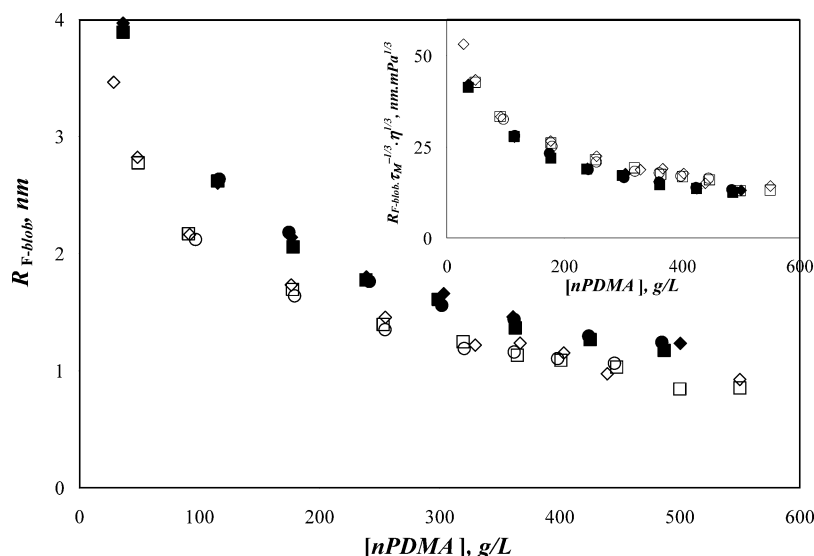


Figure 6. Plot of R_{F-blob} as a function of $nPDMA$ concentration for P265 (\diamond , \blacklozenge), P385 (\circ , \bullet), and P570 (\square , \blacksquare) in DMF (empty symbols) and acetone (full symbols). The inset is a plot of $R_{F-blob}\tau_M^{-1/3}\eta^{1/3}$ as a function of $nPDMA$ concentration.

both lifetime and viscosity combine to yield the larger R_{F-blob} found for acetone in Figure 6. Both effects should cancel out by multiplying R_{F-blob} by $\tau_M^{-1/3}$ and $\eta^{1/3}$ as done in the inset of Figure 6. The discrepancy observed between the sets of data obtained in acetone and DMF in Figure 6 is reduced in the inset, but not completely removed by taking into account the changes in lifetime and viscosity. This observation points to the fact that the assumptions made by the FBM capture the main features of the polymeric system, but that there still remains some more subtle effects which are not accounted for. One obvious effect could be differences in Py-PDMA chain conformation in acetone and DMF, respectively a poor and a good solvent for Py-PDMA.^{21,22} The Py-PDMA coil is expected to be more compact in acetone, which should affect the diffusion of the excited chromophores, and thus V_{F-blob} . Another point to consider is that the viscosity of the solvent might not be an appropriate correction factor to account for the discrepancies of R_{F-blob} in acetone and DMF in the semidilute regime, even though the relative mobility experienced by the 1-pyrenyl pendants suggests that the chromophores are still solvated by the solvent at large polymer concentrations.

In 1998, Lee and Duhamel suggested that the diffusion coefficient describing the encounters between two pyrenes attached at specific positions on a polymer backbone, i.e., the segmental diffusion coefficient D_{seg} , could be related to the rate constant of intramolecular excimer formation.²⁴ A few years later, Martinho et al. applied the same body of equations to the k_{F-blob} values obtained from the FBM for polymers randomly labeled with pyrene.^{25,26} On the basis of these considerations, eq 4 can be derived to describe how the segmental diffusion coefficient is related to k_{blob} .

$$D_{seg} = \frac{k_{F-blob} V_{F-blob}}{4\pi N_A \sigma} \quad (4)$$

The parameters N_A and σ in eq 4 are respectively the Avogadro number and the encounter radius between two pyrenes, which has been found to equal 0.8 nm.²⁷ D_{seg} was calculated by using the data provided in Figures 5 and 6 and it is shown as a function of $nPDMA$ concentration in Figure 7. All data points merge on a single master curve for $nPDMA$ concentrations larger than 150 g/L regardless of solvent or pyrene content. As the $nPDMA$ concentration nears C^* , which denotes the boundary between

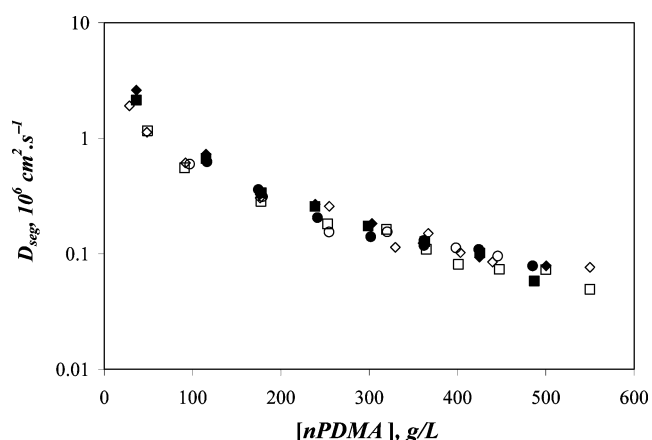


Figure 7. Plot of D_{seg} as a function of $nPDMA$ concentration for P265 (\diamond , \blacklozenge), P385 (\circ , \bullet), and P570 (\square , \blacksquare) in DMF (empty symbols) and acetone (full symbols).

the dilute and semidilute concentration regimes, D_{seg} takes values around $2-3 \times 10^{-6} \text{ cm}^2 \cdot \text{s}^{-1}$ in acetone or DMF, close to and in agreement with the value of $1.06 \times 10^{-5} \text{ cm}^2 \cdot \text{s}^{-1}$ reported for dilute solutions of poly(methyl methacrylate) in ethyl acetate.²⁸

Despite some unfortunate limitations of the present form of the FBM, it is worth noting that this set of experiments represents the first example where the encounter dynamics of pyrene pendants attached onto a polymer are described quantitatively in the semidilute regime. It is also the first example where the volume of a polymer solution probed by an excited pyrene is being determined quantitatively. This is important information for characterizing the mobility of a chromophore attached onto a polymer, which in view of the large amount of work performed with pyrene-labeled polymers has been surprisingly lacking.^{11,13,29} Many of the results obtained are internally consistent within the framework of the FBM. The volume probed by an excited pyrene decreases with increasing polymer concentration as demonstrated in Figures 4 and 6 for N_{F-blob} and R_{F-blob} in acetone and DMF. Decreasing the mobility of the chain reduces V_{F-blob} and the rate constant of encounter between two pyrenes located inside the same F-blob by the same extent resulting in k_{F-blob} remaining constant as a function of $nPDMA$ concentration (Figure 5).

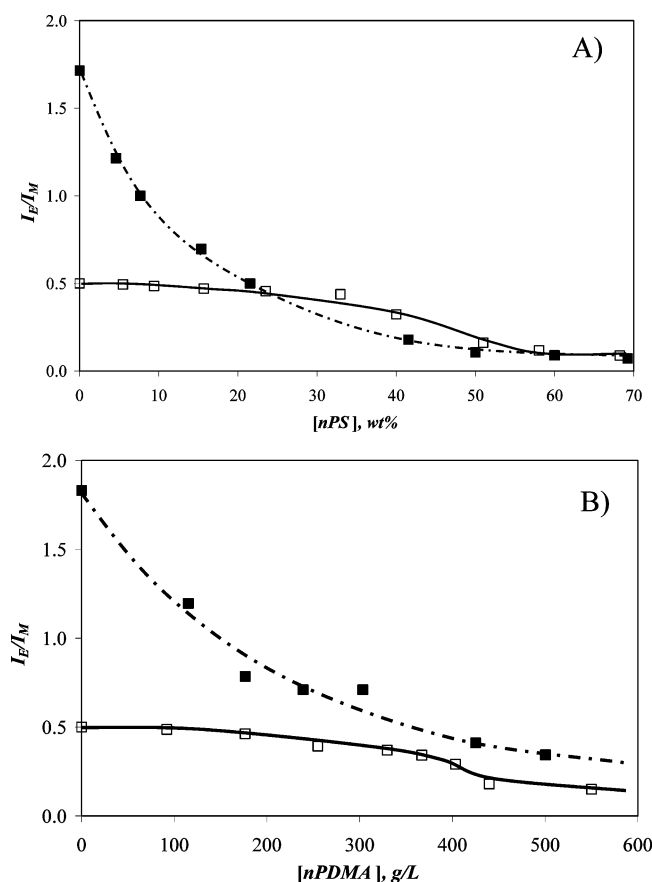


Figure 8. Plot of I_E/I_M as a function of the concentration of naked polymer. (A) Data obtained from Figure 4 in ref 16 for Py-PS in cyclopentane at 22 °C (■) and in toluene at 22 °C (□) and (B) for P265 in acetone (■) and DMF (□) at 25 °C.

Discussion

To the best of our knowledge, rather few studies have been carried out with pyrene-labeled polymers in the semidilute regime. The problems associated with these experiments have been alluded to in the Introduction. For this reason, there is only one report we are aware of that presents some qualitative information about the chain dynamics of a pyrene-labeled polystyrene (Py-PS) in the semidilute regime.¹⁶ The pyrene labels of Py-PS were located every 25–30 styrenes along the chain. The pyrene content of the Py-PS sample equalled 300 $\mu\text{mol/g}$ and its number average molecular weight, M_n , and polydispersity index, PDI, equalled 14K and 1.3, respectively. Trace amounts of Py-PS were mixed with a naked polystyrene sample, $n\text{PS}$, with M_n and PDI equal to 17.5K and 1.06, respectively. The short molecular weights used in the Py-PS study ensured that the contribution of entanglements to the chain dynamics was not important. The I_E/I_M ratio of Py-PS was obtained as a function of $n\text{PS}$ concentration at 22 °C in cyclopentane (a θ solvent for polystyrene), 2-butanone, and toluene (a good solvent for polystyrene). In Figure 8, parts A and B, the I_E/I_M ratio of Py-PS and P265 is plotted as a function of the concentration of $n\text{PS}$ and $n\text{PDMA}$, respectively. Py-PS and P265 have similar pyrene contents, but whereas the short chains of Py-PS and $n\text{PS}$ prevent the formation of entanglements, entanglements are expected to be present in the PDMA samples since they all have weight-average molecular weights larger than 100 K. In Figure 8B, the I_E/I_M ratios of P265 were normalized so that the I_E/I_M ratio of P265 in acetone equals the I_E/I_M ratio of Py-PS in cyclopentane. The plots shown in parts A and B of Figure 8 exhibit similar features. With no naked

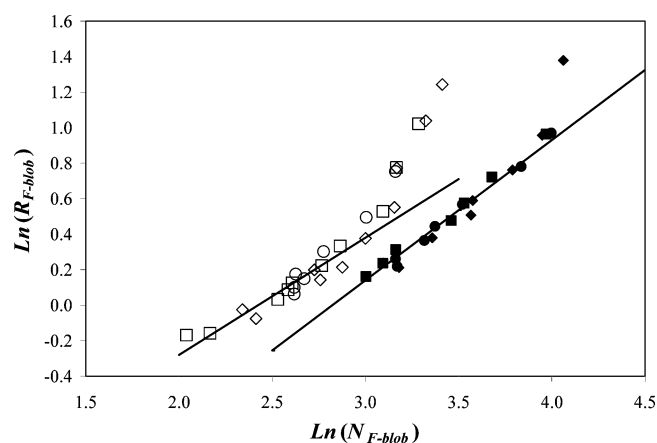
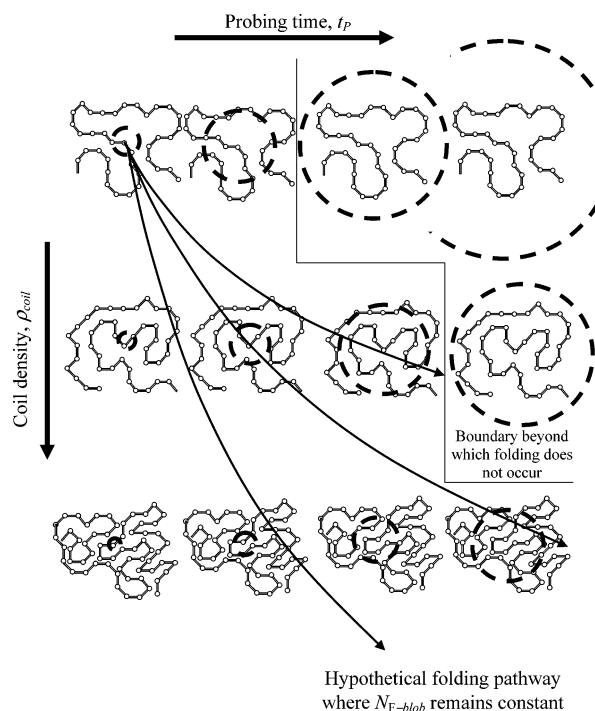


Figure 9. Plot of $\ln(R_{F\text{-blob}})$ as a function of $\ln(N_{F\text{-blob}})$ for P265 (◇), P385 (○), and P570 (□, ■) in DMF (empty symbols) and acetone (full symbols).

polymer added to the solution, the I_E/I_M ratio of both pyrene-labeled polymers is about 3.5 times larger in a θ solvent than in a good solvent. I_E/I_M decreases much more slowly with increasing concentration of the naked polymer in the good solvent than in the θ solvent. The main difference observed between the I_E/I_M trends obtained with Py-PS and P265 is the crossover found for the I_E/I_M traces of Py-PS, which is absent from the P265 sample. This discrepancy could be due to the differences in the chemical structure of the polymer backbone, the molecular weights, and the pyrene distribution along the chain of the pyrene-labeled polymers. Nevertheless and despite these differences, the overall features of the plots shown in Figure 8 are rather similar, which suggests that similar effects are being probed by the pyrene-labeled PS and PDMA polymers.

In a series of articles,^{30–35} de Gennes introduced the concept of “blob” to develop scaling relationships for polymer solutions in the semidilute regime, which helped rationalize confounding trends which had been obtained for several variables as a function of polymer concentration. Since then, blob models have been used to characterize the various properties of different polymeric systems such as linear,^{31,35} star,³⁶ and branched polymers³⁷ and block copolymers in micelles.³⁸ The hallmark of these blob models is that the radius of a “de Gennes blob”, $dG\text{-blob}$, is assumed to scale as $N_{dG\text{-blob}}^\nu$, where ν is the Flory exponent, which equals 0.5 and 0.6 in a θ and a good solvent, respectively.^{30,31} A plot of $\ln(R_{F\text{-blob}})$ vs $\ln(N_{F\text{-blob}})$ is shown in Figure 9 based on the data obtained for the Py-PDMA samples in acetone and DMF. For concentrations of $n\text{PDMA}$ larger than 100 g/L in acetone and 200 g/L in DMF, the points cluster around a straight line whose slope equals 0.79 ± 0.01 and 0.66 ± 0.03 in acetone and DMF, respectively. If a $dG\text{-blob}$ and an $F\text{-blob}$ represent similar entities, these slopes should yield the values of the Flory exponent for PDMA in acetone and DMF. The value of 0.66 ± 0.03 obtained in DMF agrees rather well with the theoretically expected value of 0.6 for a polymer in a good solvent. However, the slope of 0.79 ± 0.01 found in acetone is substantially larger than the Flory exponent of 0.5 expected in a θ solvent. For the moment, no explanation can be found for why the slope obtained in acetone is so much larger than the ν value expected for a $dG\text{-blob}$.

In an earlier paper,²² the size of an $F\text{-blob}$ was determined as a function of the lifetime of the excited pyrene. The lifetime of the excited pyrene was adjusted by adding an external quencher. As the concentration of external quencher was increased, the lifetime of pyrene was shortened and the size of an $F\text{-blob}$ decreased since the excited pyrene probed a smaller

SCHEME 1: Variation of N_{F-blob} as a Function of Probing Time and Coil Density

volume. As for all FBM studies, the present one included, the lifetime of pyrene is used as a yardstick to define the distance travelled by the excited pyrene during its lifetime.^{14,21,22} As a result, the lifetime of pyrene can be perceived as being a *probing time* and it will be referred to in such a manner in the following discussion. Rephrasing the above paragraph, the statement can now be made that the volume scanned by an excited pyrene, V_{F-blob} , during a given *probing time*, t_p , has been determined as a function of *probing time* for a polymer coil in the dilute concentration regime.²²

In the present study, V_{F-blob} has been determined as a function of polymer concentration. Since most experiments in this study were performed above C^* , the local concentration inside the polymer coil is the same as the overall polymer concentration, so that the overall polymer concentration of the solution describes the *coil density*, ρ_{coil} . The results obtained in the present study and those described in ref 22 lead to the conclusion that the size of an F-blob increases with increasing *probing time* and decreases with increasing *coil density*, as described in Scheme 1.

Scheme 1 suggests that the FBM enables the quantitative determination of the number of monomers found in the volume scanned by an excited pyrene as a function of the *coil density* and *probing time*. Consequently the FBM should be applicable to the study of phenomena where the *coil density* and *probing time* of a chain vary together. An example of such a phenomenon is a coil-to-globule transition or CGT where a polymer coil contracts over time. Scheme 1 predicts how N_{F-blob} would vary as a function of *coil density* and *probing time* during a CGT. Given a larger *probing time*, a monomer will encounter a larger number of monomers inside the polymer coil. But, as the *coil density* increases, the motion of the monomer inside the polymer coil is hindered and it will encounter fewer monomers. Thus, as a polymer coil collapses toward a more compact final state, a given monomer probes a subvolume of the polymer coil whose size increases with increasing *probing time* but decreases with increasing *coil density*. Consequently as a chain in solution folds

into a more compact conformation, both effects are expected to oppose one another.

Scheme 1 can be used to assess how N_{F-blob} could vary as a function of t_p and ρ_{coil} . If N_{F-blob} increases with increasing *probing time* much more quickly than the *coil density* increases, then a situation similar to the one shown in the top row of Scheme 1 is obtained where N_{F-blob} will grow beyond N , the number of monomers constituting the polymer, and the monomer will “escape” the polymer coil. This situation indicates that the monomer experiences too large a mobility and that a more compact conformation of the polymer coil cannot be reached. In other words, no CGT is occurring and there is no folding time to speak of. The opposite can be considered as well, where N_{F-blob} increases with increasing *probing time* much more slowly than the *coil density* increases. This situation is described in the first column of Scheme 1. Taken to its ultimate point, this path would lead to N_{F-blob} decreasing until it represents a single monomer. This is unrealistic because even in the final state of the molten globule, a monomer is expected to have enough mobility to probe over time a volume larger than its own physical boundary. What the above discussion suggests is that N_{F-blob} can neither decrease nor increase too much with t_p or ρ_{coil} . As a result, the assumption is being made hereafter that, after some transitory period, a stationary state is reached during the CGT where N_{F-blob} remains constant with t_p and ρ_{coil} and equal to N_{F-blob}^0 .

As shown in the Supporting Information, it is possible to estimate how the value of N_{F-blob}^0 affects the time taken for a CGT to occur. When N_{F-blob}^0 increases from 30 to 810, the time over which the CGT occurs increases from a few tens of microseconds to a few tens of milliseconds. According to these considerations, CGTs occurring over long time scales would be due to large N_{F-blob}^0 values. Interestingly long CGTs are observed for homopolymers, whereas short CGTs have been measured for proteins. The collapse of a homopolymer from a coil to a globule has been found to occur within 10 s, 35 s, 600 s, and 30 min for T4 DNA (166 kbp) in an aqueous solution of poly(ethylene glycol),³⁹ poly(methyl methacrylate) (PMMA) in isoamyl acetate with $M_n = 6.5 \times 10^6$,⁴⁰ polystyrene in cyclohexane with $M_w = 8.1 \times 10^6$,⁴¹ and PMMA in *tert*-butyl alcohol with $M_n = 4.1 \times 10^6$,⁴² respectively. These are indeed large CGT folding times when compared to the few tens of microseconds reported for some proteins.^{43–45} One reason the CGTs of homopolymers and proteins could occur on different time scales might be because in the case of proteins, strong specific interactions, in particular hydrophobic ones, are established between hydrophobic amino acids. These interactions generate transient cross-links which restrict the motion of the monomers. Consequently, small N_{F-blob}^0 values are expected for the CGT of proteins thereby leading to CGTs occurring over short time scales.

Certainly there are many proteins whose CGT occurs on a submillisecond time scale.^{43–49} Proteins such as cytochrome *c* have been found to collapse within a few tens of microseconds.^{39–41} A fast collapse to the molten globule has also been suggested from theoretical considerations.^{50,51} Such a fast collapse would be observed for the smaller N_{F-blob}^0 values used in Figure SI.1 in the Supporting Information, namely, $N_{F-blob}^0 = 30$. An F-blob made of 30 units for a polymer in a collapsed globule is actually reasonable considering that a compact α -helical poly(L-glutamic acid) randomly labeled with pyrene has been shown to yield an N_{F-blob}^0 value of 31 amino acids.⁵² Thus if a value of 30 were arbitrarily chosen for N_{F-blob}^0 , the above discussion would lead to the conclusion that each

monomer of the chain would interact with the 30 other ones located inside an F-blob while the chain undergoes a CGT. Since this $N_{\text{F-blob}}^0$ value is rather small, a fast CGT would be expected. That this might be the case could also have further implications for the subsequent steps of the folding of a protein when it proceeds from the disordered molten globule to its final 3-D structure because this process should involve subdomains made of $N_{\text{F-blob}}^0 = 30$ or even fewer monomers. A hypothetical polypeptidic chain made of 300 monomers could then be arbitrarily divided into 10 F-blobs made of 30 monomers inside which folding would occur. If each monomer had two degrees of freedom and was given 10^{-13} s to sample any conformation inside an F-blob,⁵³ then the total folding time for this hypothetical chain would be obtained from $10 \times 2N_{\text{F-blob}}^0 \times 10^{-13}$ s = 1.1 ms with $N_{\text{F-blob}}^0 = 30$. A 1 ms folding time is very reasonable for a 300 amino acid-long protein when compared to the folding time that would be expected if that 300 monomer-long chain were not compartmentalized into 10 F-blobs. Without compartmentalization, the folding time would have been $2^{300} \times 10^{-13}$ s = 6.5×10^{69} years, an impossible folding time since most proteins are known to fold within a few milliseconds to seconds.

The impossibly long folding time resulting from the sampling of all possible conformations of a 300 monomer-long chain is known as Levinthal's paradox.⁵³ It demonstrates that protein folding does not occur via an all-out sampling of the entire conformation space. Levinthal's paradox has prompted scientists to imagine pathways that would allow a polymeric chain to decrease the vast conformation space the chain needs to sample before reaching its active final structure. Such pathways include the "framework model",⁵⁴ the "nucleation model",^{55,56} the "hydrophobic-collapse model",⁵⁷ or a folding where the search of the conformational space is constrained by "energy funnels".^{58,59} The present work suggests that an approach based on *probing time*- and *coil density*-dependent blobs could also result in reasonable folding times for proteins. It remains to be seen whether such blob-based approaches could contribute to improving our understanding of protein folding.

Conclusions

Three PDMA chains internally and randomly labeled with pyrene were used to monitor the dynamics of PDMA chains in the semidilute regime in acetone and DMF. These experiments were carried out with solutions containing trace amounts of Py-PDMA and increasing concentrations (0–550 g/L) of naked PDMA. The extremely low Py-PDMA concentration ensures that the fluorescence measurements report on the intramolecular formation of the pyrene excimer. Although the macroscopic viscosity of the solution increases drastically with increasing polymer concentration, the steady-state and time-resolved fluorescence experiments indicate that the pyrene labels experience locally substantial mobility (Figure 2). The fluorescence data were analyzed in terms of a FBM, which provided the number of monomers making up the volume $V_{\text{F-blob}}$ probed by an excited pyrene during its lifetime. This number, referred to as $N_{\text{F-blob}}$, decreases with increasing polymer concentration (Figure 4) and so did $R_{\text{F-blob}}$ (Figure 6). This behavior reflects the reduced mobility of pyrene upon increasing the polymer concentration. At any polymer concentration, $N_{\text{F-blob}}$ and $R_{\text{F-blob}}$ were larger in acetone than in DMF. This observation is due to the smaller viscosity of acetone and the larger lifetime of the 1-pyrenyl chromophore in acetone which both allow the excited chromophore to probe a larger volume. Of particular interest,

the volume probed by the excited 1-pyrenyl pendant in a polymer solution was determined quantitatively for the first time.

The results obtained in the present report were also compared with those of an earlier publication.¹⁶ It was found that the trends obtained for the I_E/I_M ratio of the pyrene-labeled polymers versus the concentration of naked polymer were very similar whether the experiments were performed with Py-PDMA in acetone and DMF at 25 °C and Py-PS in cyclopentane and toluene at 22 °C (cf. Figure 8A,B). This observation supports the claim that the behavior observed with the Py-PDMA or Py-PS samples is general. The scaling laws expected to hold for blob models describing the behavior of polymers in the semidilute regime were investigated. They were poorly obeyed in acetone but relatively well obeyed in DMF where $R_{\text{F-blob}}$ was found to scale as $N_{\text{F-blob}}^\nu$ where ν equals 0.66 ± 0.03 , which is close to the expected Flory exponent value of 0.6 for a polymer in a good solvent.

Suggestions were made on how the results of this study could be used to provide some insight about some of the factors that could control the time scale over which a polymer undergoes a CGT. During a CGT, the size of the polymer coil decreases with time as the solvent quality toward the polymer worsens. It was proposed that as time elapses during a CGT, $N_{\text{F-blob}}$ increases with increasing time and decreases with increasing coil density. The assumption was made that, after some transitory period, both effects cancel each others so that $N_{\text{F-blob}}$ remains constant and equal to $N_{\text{F-blob}}^0$ during a CGT. A derivation is suggested in the Supporting Information that yields the time required for a polymer coil to undergo a CGT. It was found to depend strongly on $N_{\text{F-blob}}^0$. Small $N_{\text{F-blob}}^0$ values yield rapid CGTs occurring within tens of microseconds whereas large $N_{\text{F-blob}}^0$ values result in much slower CGTs. These predictions suggest that FBM studies on pyrene-labeled polymers might provide new insights for the investigation of the CGTs of polymers, and maybe the folding of proteins.

Acknowledgment. J.D. is thankful to Prof. M. A. Winnik from the University of Toronto for suggesting applying the FBM to the study of pyrene-labeled polymers in the semidilute regime. J.D. is also thankful to funding from NSERC and CFI, as well as to his award of a Tier-2 Canada Research Chair.

Supporting Information Available: The parameters retrieved from the analysis of the fluorescence decays with eq 1 (Tables SI.1 and SI.2), the slope and intercept of the straight lines that fit $N_{\text{F-blob}}$ as a function of polymer concentration and lifetime of the 1-pyrenyl pendant (Table SI.3), estimates of the time needed for a CGT to occur as a function of $N_{\text{F-blob}}^0$ (Table SI.4), and the derivation of a relationship between the probing time and coil density is given for different $N_{\text{F-blob}}^0$ values. This material is available free of charge via the Internet at <http://pubs.acs.org>.

References and Notes

- (1) Chung, G.-C.; Kornfield, J. A.; Smith, S. D. *Macromolecules* **1994**, *27*, 964–973.
- (2) Chung, G.-C.; Kornfield, J. A.; Smith, S. D. *Macromolecules* **1994**, *27*, 5729–5741.
- (3) Destrée, M.; Laupêtre, F.; Lyulin, A.; Ryckaert, J.-P. *J. Chem. Phys.* **2000**, *112*, 9632–9644.
- (4) Floudas, G.; Reisinger, T. *J. Chem. Phys.* **1999**, *111*, 5201–5204.
- (5) Floudas, G.; Gravalides, C.; Reisinger, T.; Wegner, G. *J. Chem. Phys.* **1999**, *111*, 9847–9852.
- (6) Viovy, J. L.; Frank, C. W.; Monnerie, L. *Macromolecules* **1985**, *18*, 2606–2613.
- (7) Jarry, J. P.; Erman, B.; Monnerie, L. *Macromolecules* **1986**, *19*, 2750–2755.

- (8) Punchard, B. J.; Adolf, D. B. *J. Chem. Phys.* **2002**, *117*, 774–7780.
- (9) Kirpatch, A.; Adolf, D. B. *Macromolecules* **2004**, *37*, 1576–1582.
- (10) Adams, S.; Adolf, D. B. *Macromolecules* **1998**, *31*, 5794–5799.
- (11) Winnik, M. A. *Acc. Chem. Res.* **1985**, *18*, 73–79.
- (12) Morawetz, H. *J. Lumin.* **1989**, *43*, 59–71.
- (13) Duhamel, J. *Molecular Interfacial Phenomena of Polymers and Biopolymers*; Chen, P., Ed.; Woodhead: New York, 2005; pp 214–248.
- (14) Mathew, A.; Siu, H.; Duhamel, J. *Macromolecules* **1999**, *32*, 7100–7108.
- (15) Winnik, M. A.; Egan, L. S.; Tencer, M.; Croucher, M. D. *Polymer* **1987**, *28*, 1553–1560.
- (16) Winnik, M. A.; Li, X.-B.; Guillet, J. E. *Macromolecules* **1984**, *17*, 699–702.
- (17) Cheung, S.-T.; Winnik, M. A.; Redpath, A. E. C. *Makromol. Chem.* **1982**, *183*, 1815–1824.
- (18) Fields, S. *Science* **2001**, *291*, 1221–1224.
- (19) Tachiya, M. *Chem. Phys. Lett.* **1975**, *33*, 289–292.
- (20) Infelta, P. P.; Gratzel, M.; Thomas, J. K. *J. Phys. Chem.* **1974**, *78*, 190–195.
- (21) Kanagalingam, S.; Ngan, C. F.; Duhamel, J. *Macromolecules* **2002**, *35*, 8560–8570.
- (22) Kanagalingam, S.; Spartalis, J.; Cao, T.-M.; Duhamel, J. *Macromolecules* **2002**, *35*, 8571–8577.
- (23) Regalado, E. J.; Selb, J.; Candau, F. *Macromolecules* **1999**, *32*, 8580–8588.
- (24) Lee, S.; Duhamel, J. *Macromolecules* **1998**, *31*, 3–9200.
- (25) Picarra, S.; Relogio, P.; Afonso, C. A. M.; Martinho, J. M. G.; Farinha, J. P. S. *Macromolecules* **2003**, *36*, 8119–8129.
- (26) Picarra, S.; Duhamel, J.; Fedorov, A.; Martinho, J. M. G. *J. Phys. Chem. B* **2004**, *108*, 12009–12015.
- (27) Duhamel, J.; Winnik, M. A.; Baros, F.; André, J. C.; Martinho, J. M. G. *J. Phys. Chem.* **1992**, *96*, 9805–9810.
- (28) Winnik, M. A.; Pekcan, O.; Egan, L. *Polymer* **1984**, *25*, 1767–1773.
- (29) Winnik, F. M. *Chem. Rev.* **1993**, *93*, 587–614.
- (30) de Gennes, P.-G. *Macromolecules* **1976**, *9*, 587–593.
- (31) de Gennes, P.-G. *Macromolecules* **1976**, *9*, 594–598.
- (32) Brochard, F.; de Gennes, P.-G. *Macromolecules* **1977**, *10*, 1157–1161.
- (33) de Gennes, P.-G. *Scaling Concepts in Polymer Physics*; Cornell University: Ithaca, NY, 1979.
- (34) Cotton, J. P.; Nierlich, M.; Boué, F.; Daoud, M.; Farnoux, B.; Jannink, G.; Duplessix, R.; Picot, C. *J. Chem. Phys.* **1976**, *65*, 1101–1108.
- (35) Daoud, M.; Cotton, J. P.; Farnoux, B.; Jannink, G.; Sarma, G.; Benoit, H.; Duplessix, R.; Picot, C.; de Gennes, P. G. *Macromolecules* **1975**, *8*, 804–818.
- (36) Daoud, M.; Cotton, J. P. *J. Phys. (Paris)* **1982**, *43*, 531–538.
- (37) Daoud, M.; Joanny, J. F. *J. Phys. (Paris)* **1981**, *42*, 1359–1371.
- (38) Halperin, A. *Macromolecules* **1987**, *20*, 2943–2946.
- (39) Yoshikawa, K.; Matsuzawa, Y. *J. Am. Chem. Soc.* **1996**, *118*, 929–930.
- (40) Kayaman, N.; Gürel, E.; Baysal, B. M.; Karasz, F. E. *Macromolecules* **1999**, *32*, 8399–8403.
- (41) Chu, B.; Ying, Q. C.; Grosberg, A. Y. *Macromolecules* **1995**, *28*, 180–189.
- (42) Nakamura, Y.; Sasaki, N.; Nakata, M. *J. Chem. Phys.* **2003**, *118*, 3861–3866.
- (43) Shastry, M. C. R.; Roder, H. *Nature Struct. Biol.* **1998**, *5*, 385–392.
- (44) Hagen, S. J.; Eaton, W. A. *J. Mol. Biol.* **2000**, *301*, 1019–1027.
- (45) Qiu, L.; Zachariah, C.; Hagen, S. J. *Phys. Rev. Lett.* **2003**, *90*, 1–4.
- (46) Eaton, W. A.; Muñoz, V.; Thompson, P. A.; Chan, C.-K.; Hofrichter, J. *Curr. Opin. Struct. Biol.* **1997**, *7*, 10–14.
- (47) Yang, W. Y.; Gruebele, M. *Nature* **2003**, *423*, 193–197.
- (48) Ballew, R. M.; Sabelko, J.; Gruebele, M. *Proc. Natl. Acad. Sci. U.S.A.* **1996**, *93*, 5759–5764.
- (49) Sadqi, M.; Lapidus, L. J.; Muñoz, V. *Proc. Natl. Acad. Sci. U.S.A.* **2003**, *100*, 12117–12122.
- (50) Thirumalai, D. *J. Phys. I* **1995**, *5*, 1457–1467.
- (51) Pitard, E.; Orland, H. *Eur. Phys. Lett.* **1998**, *41*, 467–472.
- (52) Duhamel, J.; Kanagalingam, S.; O'Brien, T.; Ingratta, M. *J. Am. Chem. Soc.* **2003**, *125*, 12810–12822.
- (53) Stryer, L. *Biochemistry*; W. H. Freeman and Company: New York, 1995; p 418.
- (54) Ptitsyn, O. B. *Protein Eng.* **1994**, *7*, 593–596.
- (55) Wetlaufer, D. B. *Proc. Natl. Acad. Sci. U.S.A.* **1973**, *70*, 697–701.
- (56) Wetlaufer, D. B. *Trends Biochem. Sci.* **1990**, *15*, 414–415.
- (57) Dill, K. A.; Bromberg, S.; Yue, K.; Fiebig, K. M.; Yee, D. P.; Thomas, P. D.; Chan, H. S. *Protein Sci.* **1995**, *4*, 561–602.
- (58) Dill, K. A.; Chan, H. S. *Nature Struct. Biol.* **1997**, *4*, 10–19.
- (59) Dinner, A. R.; Šali, A.; Smith, L. J.; Dobson, C. M.; Karplus, M. *Trends Biochem. Sci.* **2000**, *25*, 331–339.